

<Research Paper>

## Particle Size, Morphology and Color Characteristics of C.I. Pigment Red 57:1 : 1. Effect of Synthesis Conditions

Hee Sung Seo, Hyun Kyung Lee<sup>1</sup> and Eui Sang Yoo<sup>1,†</sup>

Department of Clothing and Textiles, Ewha Womans University, Seoul, Korea

<sup>1</sup>Human and Culture Convergence Technology R&D Group, Korea Institute of Industrial Technology, Ansan, Korea

(Received: October 12, 2015 / Revised: November 24, 2015 / Accepted: December 01, 2015)

**Abstract:** The effects of synthesis conditions on characteristics of the calcium-azo complex pigment, C.I. Pigment Red 57:1, were studied. It was mainly considered that the industrially required synthesis conditions for lowering electrical conductivity of the pigment solution keeping pigment quality such as particle size and color characteristics. Three parameters were chosen as control factors during the synthesis. The first was the amount of hydrochloric acid added to transform sodium nitrite into nitrous acid. The second was the amount of calcium chloride added to insolubilize the synthesized azo dye. The final factor was pH control during the coupling reaction. The electrical conductivity and pigment aggregate particle size were dependent on the amount of hydrochloric acid and calcium chloride. Higher HCl concentration gave brighter yellowish-red color because of smaller particle aggregate size and narrower size distribution. Amount of charged ions in the synthesis process might affect the “lake” formation resulting different particle aggregate size and color shade.

**Keywords:** C.I. Pigment Red 57:1, synthesis conditions, electrical conductivity, particle size, color characteristics

### 1. Introduction

Compared to dyes, organic pigments have been more intensively studied and developed in recent years. They have been applied not only in printing inks, paints, plastics, and coatings, but also, via the development of novel functional pigments, in high-technology industries such as IT (information technology), energy and electronic industries. Environmental concern about inorganic pigments containing heavy metals has increased the interest on organic pigments recently.

And even in the organic pigment industry, eco-friendly synthesis process has been preferred because of less amounts of waste water or chemical.

To this purpose, this paper proposes an optimized manufacturing process for one of organic pigments, the calcium-complex azo pigment denoting as C.I. Pigment

Red 57:1.

C.I. Pigment Red 57:1 (so-called PR 57:1, Lithol Rubine, Ca4B, or C.I. No.15850:1) has been one of the most important and popular organic red pigment. It is normally used as a standard magenta color for multi-color printing because of its intense bluish red tint<sup>1-4</sup>. This pigment is generally known as one of  $\beta$ ONA pigments, for beta-oxynaphthoic acids, which precipitate as calcium salts especially with 2-hydroxy-3-naphthoic acid; i.e., the 1:1 calcium salt of 4-(4-methyl-2-sulfo-phenyl) azo-3-hydroxy-2-naphthalic acid<sup>1-6</sup>.

They organically chelate with calcium to form insoluble complexes or lakes. It is known that this chelate form has excellent brilliance and transparency, high tint strength, and good solvent and heat resistance<sup>1-4</sup>. Recently, they are applied in toners for electrophotographic system, and in ink-jet printing inks<sup>4,7</sup>.

The preparation of C.I. Pigment Red 57:1 (PR 57:1) involves the diazotization of 2-amino-5-methyl benzene sulfonic acid (4B acid) and a subsequent coupling

<sup>†</sup>Corresponding author: Eui Sang Yoo (esyoo@kitech.re.kr)  
© 2015 The Korean Society of Dyers and Finishers.  
All rights reserved. TCF 27-4/2015-12/229-244

reaction with 3-hydroxy-2-naphthoic acid (BON-acid), under alkaline conditions<sup>1-5)</sup>. The resultant disodium salt is converted to the calcium salt, e.g., with calcium chloride.

The synthesis conditions for this azo pigment have an important influence on the physical properties such as particle size/size distribution, morphology, and ultimately, on the application of the pigment<sup>1,8,9)</sup>.

However, there are few studies on the effects of the conditions during synthesis of the PR 57:1 on the particles converted to the calcium salt.

This paper studied the characteristics of PR 57:1 transformed to the calcium salt, and focused on the effects of the reaction conditions during the diazotization, coupling, and calcium salt conversion processes. Three parameters of synthesis were selected:

The amount of hydrochloric acid (HCl) in the diazotization process was controlled. HCl reacts with sodium nitrite (NaNO<sub>2</sub>) to form nitrous acid (HNO<sub>2</sub>) which is used to diazotize the 4B acid.

The amount of calcium chloride (CaCl<sub>2</sub>) was controlled. CaCl<sub>2</sub> is used to make the azo dye insoluble in the coupling reaction, being "laking". The amount of CaCl<sub>2</sub> actually effects the conversion to the calcium salt of the pigment particles.

The pH value during the coupling reaction at the laking step was controlled.

The pH balance during the final coupling reaction was so important in the conversion to the calcium salt of the particles. The pH conditions can determine the aggregate structure and morphology of the pigment particles.

The pigments prepared under these varied conditions were compared to each other. Characteristics of the pigments, i.e., particle/aggregate size, morphology and color variations, were evaluated and the electrical conductivity of pigment solution were characterized. High electrical conductivity of pigment solution means high ion concentration residue after synthesis reaction and makes the ink spread on the printing boundary during printing.

And the salts causing high electrical conductivity also become issues of wastewater.

In the industry, it is so important to maintain the consistent color characteristics of pigments on every batch reaction. The color characteristics of pigments depend on the particle/aggregate size and morphology, size distribution, dispersibility as well as on the chemical structure.

In general, the crude pigment is not used directly from synthesis. The post-synthesis process such as milling and surface treatment is operated to improve dispersity and color properties. In this work, we studied on the color characteristics of PR 57:1 in terms of size and morphology of the particle aggregates before post-synthesis process.

In another series of this work, how to affect the milling process on the color characteristics of PR 57:1 was studied and reported.

We have focused on the interpretation of the influence of acid/CaCl<sub>2</sub> concentration and the cause of changes in particle aggregate size and color values by chemical factors such as protons or calcium ions present during the metal-pigment complex formation. The results on the consideration of the relationship between synthesis condition and the pigments characteristics can help to design the manufacturing process in industry for better maintenance of the pigment quality.

## 2. Experimental

### 2.1 Synthesis of PR 57:1

All reagents used for the synthesis of PR 57:1 were kindly donated by Ukseung Chemical Co., Ltd.

The synthetic scheme for PR 57:1 (1) is illustrated in Figure 1.

The synthesis was conducted through diazotization of 4B acid (2) followed by coupling with BON-acid (3), which affords the soluble sodium salt form. Subsequent reaction with calcium chloride under alkaline condition yields the insoluble calcium salt (pigment-lake) form<sup>1,5,10)</sup>.

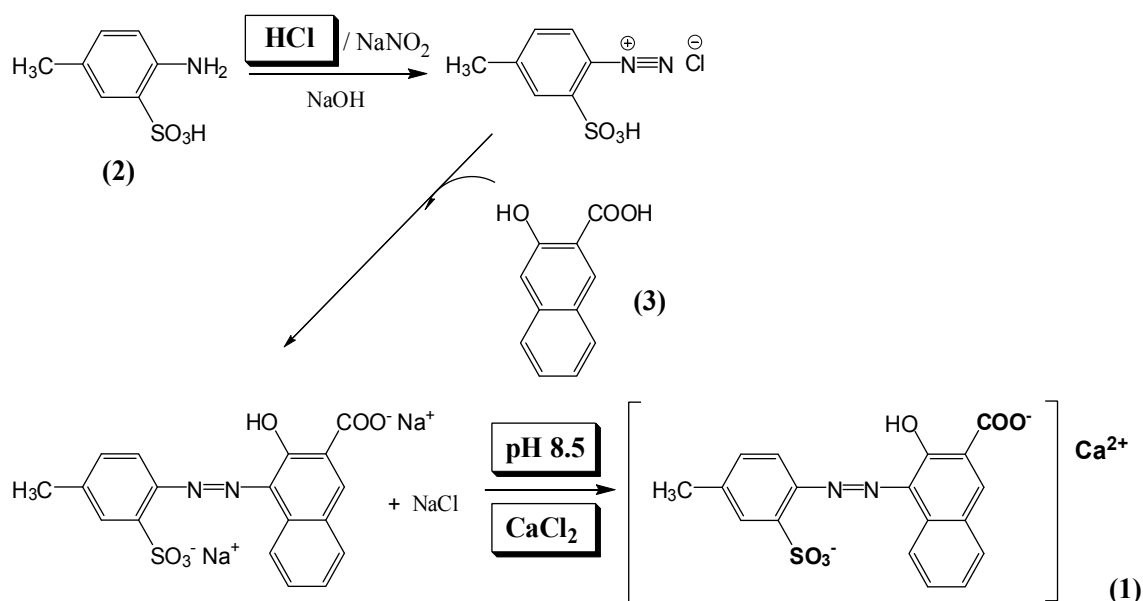


Figure 1. Synthetic scheme for C.I. Pigment Red 57:1.

The reaction was carried out as follows and amount chemicals in the description are for the standard reaction: 4B acid (2) (88.8g, 0.474mol) was dissolved into a solution of sodium hydroxide (50% NaOH, 38.8g) in water (1ℓ) [4B acid dissolution process]. The resulting brown solution was cooled down below 5°C using ice and concentrated hydrochloric acid (adjusted 22% HCl, 136ml, as standard condition) was added. A solution of sodium nitrite (NaNO<sub>2</sub>: 34.6g, 0.501mol, dissolved in 500ml water) was added and the suspension stirred for 15min below 5°C. After confirming the presence of excess nitrous acid of sodium nitrite by starch-KI paper (turned into a deep blue violet color), aqueous HCl solution was dropping until the excess nitrous acid was disappeared just before the coupling. When the pale brown suspension appeared from the homogeneous mixture, the addition of HCl was completed followed by stirring for further 30min [diazotization reaction].

Separately BONA-acid (3) (89.2g, 0.474mol) was dissolved in a solution of sodium hydroxide (50% NaOH, 43.3g) in water (1ℓ) [coupler dissolution]. The light-brown solution was then cooled to 15°C while stirring vigorously.

The resultant diazonium salt suspension was added slowly to the prepared coupler solution. The color changed initially to a dark red solution, and finally to a yellowish red (orange) which is the color of

precipitated dyestuff. The mixture was stirred for more than 2hour at room temperature [coupling reaction]. During the preparing the orange solution of sodium salt dyes, the pH level was adjusted as 8.5 (as standard condition) using a 2M solution of sodium hydroxide. A solution of calcium chloride (CaCl<sub>2</sub>: 95.6g, in 500ml water, as standard condition) was added and stirred for 15min at room temperature to make an insoluble calcium salt [Ca-lake formation]. The absence of excess diazonium salt was checked using H-acid spot test<sup>(1)</sup>. The suspension was isolated by filtration and washed with deionized water several times to remove excess inorganic salt by-product, and finally dried at room temperature.

In the synthesis process explained above, the amounts of the HCl and CaCl<sub>2</sub> were varied with a certain level: the HCl and CaCl<sub>2</sub> concentrations were increased or decreased by 10% from the standard amounts of the HCl and CaCl<sub>2</sub> used. The 10% variation means 149.6ml or 122.4ml of 22% HCl solution and 105.16g or 86.04g of CaCl<sub>2</sub> in 500ml water which are determined on the basis of the stoichiometric amount of 4B acid (88.8g, 0.474mol) and BONA-acid (89.2g, 0.474mol). Besides chemical amount, the pH value during the coupling reaction was controlled at three levels of 7.5, 8.5, and 9.5

by decreasing or increasing alkalinity.

The sample codes for the synthesized pigments are listed in Table 1, with the each synthesis conditions. In the table, the designation of '0' means the amount of HCl or CaCl<sub>2</sub> in standard reaction described in detail above.

## 2.2 Measurements of properties

Synthesized PR 57:1 suspensions were prepared to measure ion conductivity and particle size. Sonication treatment was used for dispersion of the pigments temporarily before particle size analysis.

The electrical conductivity of the synthesized pigment suspension was determined using a conductivity meter (HI-9932, Hanna Instruments, USA). The pigment suspensions for electrical conductivity measurement were prepared by filtering, washing, drying and redispersing in water before final drying, for excluding the presence of the Na<sup>+</sup>, Ca<sup>++</sup> and Cl<sup>-</sup> ions in the suspension which are derived from the HCl, NaOH, and CaCl<sub>2</sub> used in the synthesis process, which influence the conductivities. The NaCl (and the excess of CaCl<sub>2</sub>) in the suspensions was removed by washing with deionized water several times before the conductivity analysis.

The pigment suspensions were adjusted to 25°C and conductivity was measured 3 times with 60 seconds

interval to get the reproducible conductivities.

The particle sizes (obviously the size of the particle agglomerates or aggregates) of the synthesized pigments before drying were measured using a particle size analyzer (LS<sup>TM</sup> 13 320 Particle Size Analyzer, Beckman Coulter Inc., USA). The pigment solutions were diluted 100-fold in distilled water and sonicated for 2h with an ultrasonicator before observation.

The scanning electron microscope analysis was performed using a scanning electron microscope (JSM-5510, JEOL Co., Japan). For the sample preparation, all pigment samples were dispersed ultrasonically in distilled water. One droplet of the solution was placed on a piece of silicon wafer using a Pt wire, and the solvent was evaporated at room temperature. The micrographs of all samples were obtained with an exposure time of 4s at a magnification of 5,000.

Pigment samples were pulverized and mixed with mineral oil varnish. 1.2g of pigment was mixed with 0.2g of mineral oil varnish, and the color mixture was painted on a piece of white paper (5×5cm) using a doctor blade<sup>12)</sup>. This painted paper was then covered with a transparent OHP film for diffusion control, and dried before measuring the color. The dried-paint films were tested by color measurement, using the CIE 1976 L\*a\*b\* method<sup>12)</sup> by computer color

**Table 1.** Sample codes for synthesized pigments with respective synthesis conditions

No.	HCl	CaCl <sub>2</sub>	pH	No.	HCl	CaCl <sub>2</sub>	pH	No.	HCl	CaCl <sub>2</sub>	pH
1	-10%	-10%	7.5	10	0	-10%	7.5	19	+10%	-10%	7.5
2	-10%	-10%	8.5	11	0	-10%	8.5	20	+10%	-10%	8.5
3	-10%	-10%	9.5	12	0	-10%	9.5	21	+10%	-10%	9.5
4	-10%	0	7.5	13	0	0	7.5	22	+10%	0	7.5
5	-10%	0	8.5	14	0	0	8.5	23	+10%	0	8.5
6	-10%	0	9.5	15	0	0	9.5	24	+10%	0	9.5
7	-10%	+10%	7.5	16	0	+10%	7.5	25	+10%	+10%	7.5
8	-10%	+10%	8.5	17	0	+10%	8.5	26	+10%	+10%	8.5
9	-10%	+10%	9.5	18	0	+10%	9.5	27	+10%	+10%	9.5

matching (CCM) (Color-eye<sup>®</sup> 3100, Gretag Macbeth Co., USA) with illuminant D<sub>65</sub>/10°.

A chromatic difference value ( $\Delta E$ ), as a magnitude of color difference, were also measured, using obtained variables of  $L^*a^*b^*$  values between a pigment under the standard condition and the modified pigments under changed conditions. The value of  $\Delta E$  is determined by the following equation(1)<sup>13)</sup>.

$$\Delta E = \{(L^*_1 - L^*_2)^2 + (a^*_1 - a^*_2)^2 + (b^*_1 - b^*_2)^2\}^{1/2} \dots \dots \dots (1)$$

where,

$\Delta E$  : A chromatic difference value

$L^*$  : Whiteness

$a^*$  : Redness

$b^*$  : Yellowness

1 : Standard pigment

2 : Modified pigment

### 3. Results and Discussion

The influence of change of synthesis condition on pigment properties was easily explained by understanding the mechanism for the formation of a meta l-pigment complex and its structure.

In the calcium lake pigment of PR 57:1, calcium atoms are positioned at the center of the complex, enhancing affinity through the chelation of two ligands in the pigment molecule, the sulfonate ( $\text{SO}_3^-$ ) group on the diazo component and the carboxylate ( $\text{CO}_2^-$ ) group on the coupling component<sup>4)</sup>. This form allows the pigment to precipitate in an insoluble form and to be transformed into a nonelectrolyte in the Ca-pigment complex. Because the ionic interactions are both intermolecular and intramolecular, the pigments are associated as ion pairs of  $\text{Ca}^{2+}$  with  $\text{SO}_3^-$  and  $\text{CO}_2^-$  groups in the pigment molecules.

Pigments of this type are known to exist largely in the ketohydrazone form<sup>4,6,14)</sup>. Deprotonation occurs at both the sulfonate and carboxylate groups but not at the hydroxy or hydrazo groups, and there is only one type of calcium binding site<sup>6)</sup>.

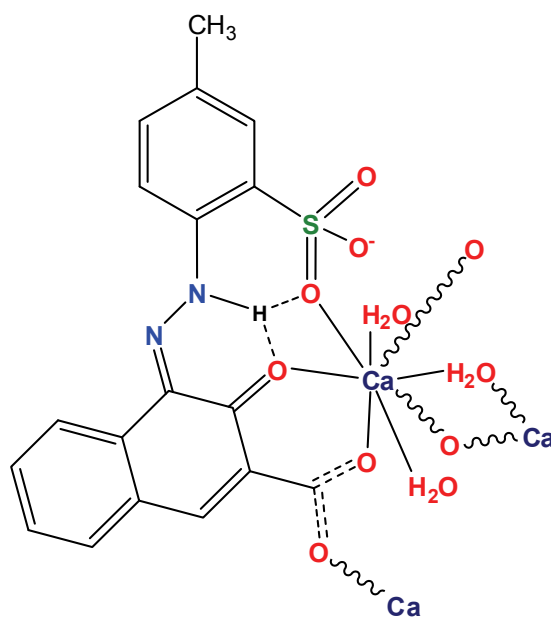


**Figure 2.** Molecular coordination geometry about Ca in C.I. Pigment Red 57:1, e.g., trihydrate form in synthesis.

The calcium atom is significantly placed in the ligand plane as shown in Figure 2. The Ca atoms are properly eight-coordinate, bonding to the three carboxylate, keto, and sulfonate sites on one azo anion, two terminal water molecules, and three bridging oxygen atoms supplied by the carboxylate groups of neighboring azo anions<sup>4,6)</sup>. Judging from the planar conjugated system featuring C=O and NH functional groups in the pigments<sup>15)</sup>, they may adopt a structure of chromophores stacked in parallel.

The pigments crystallize during construction of the molecular assembly, forming a double-layer structure toward a highly anisotropic crystal structure.

The crystal structure and the packing properties in PR 57:1 had been recently elucidated by Bekö, et al.<sup>16)</sup>, in contrast to the older hypotheses regarding a zigzag ladder-like system in a head-to-tail arrangement (Duckett, et al.)<sup>17)</sup> or a polymeric double-chain structure of Ca atoms (Harris, et al.)<sup>14)</sup>. From the work of Bekö et al.<sup>16)</sup>, it is known that PR 57:1 exists in three different crystal phases with different colors:

In the synthesis, the carmine-red alpha-phase(trihydrate) is formed; heating to 50°C leads to the magenta

beta-phase (monohydrate); heating to 200°C leads to the dull dark magenta anhydrate.

Industrially the beta-phase is used because of the standard magenta shade. The presence and position of the ionic groups in pigment molecules and the process which metal ions bond to the anions via electrostatic interactions could play an important role in determining ionic conductivity, as well as in determining the assembly of the particles<sup>18)</sup>, crystallization behaviors, particle sizes and distributions, and the final colors.

The acidity of HCl favors the formation of  $\text{NO}^+$ , generated by reaction with sodium nitrite, and facilitates the formation of the strongly electrophilic diazonium ions,  $\text{ArN}_2^+$ , for a more rapid coupling process<sup>19)</sup>. The sodium salt of the PR 57:1 is formed through the coupling process.

In the salt form, sodium cations associated with the  $\text{SO}_3^-$  and  $\text{CO}_2^-$  anions encourage water solubility.

The compound is transformed into a water-insoluble calcium salt form during “lake” formation, by replacement of the two sodium cations with divalent calcium cations.

The amount of  $\text{CaCl}_2$  influences the Na-to-Ca metal-exchange process. The pH (hydrogen ion concentration) finally determines the degree of conversion into the calcium salt form by changing the extent of protonation in the two salt-forming acidic groups (sulfonate and carboxylate)<sup>20)</sup>. The mechanism of complex formation depends on the appropriate amount of HCl as well as  $\text{CaCl}_2$  used. Particularly in a 1:1 molar ratio of  $\text{SO}_3^-$  and  $\text{CO}_2^-$  anions and  $\text{Ca}^{2+}$  cation, the calcium salt is immediately precipitated from solution with stabilized electrical charge<sup>21)</sup>, to finally form the neutralized “lake”.

In Figures 3a, 3b, and 3c, the effects of HCl and  $\text{CaCl}_2$  concentrations on the electrical conductivity are demonstrated under different pH conditions (7.5,

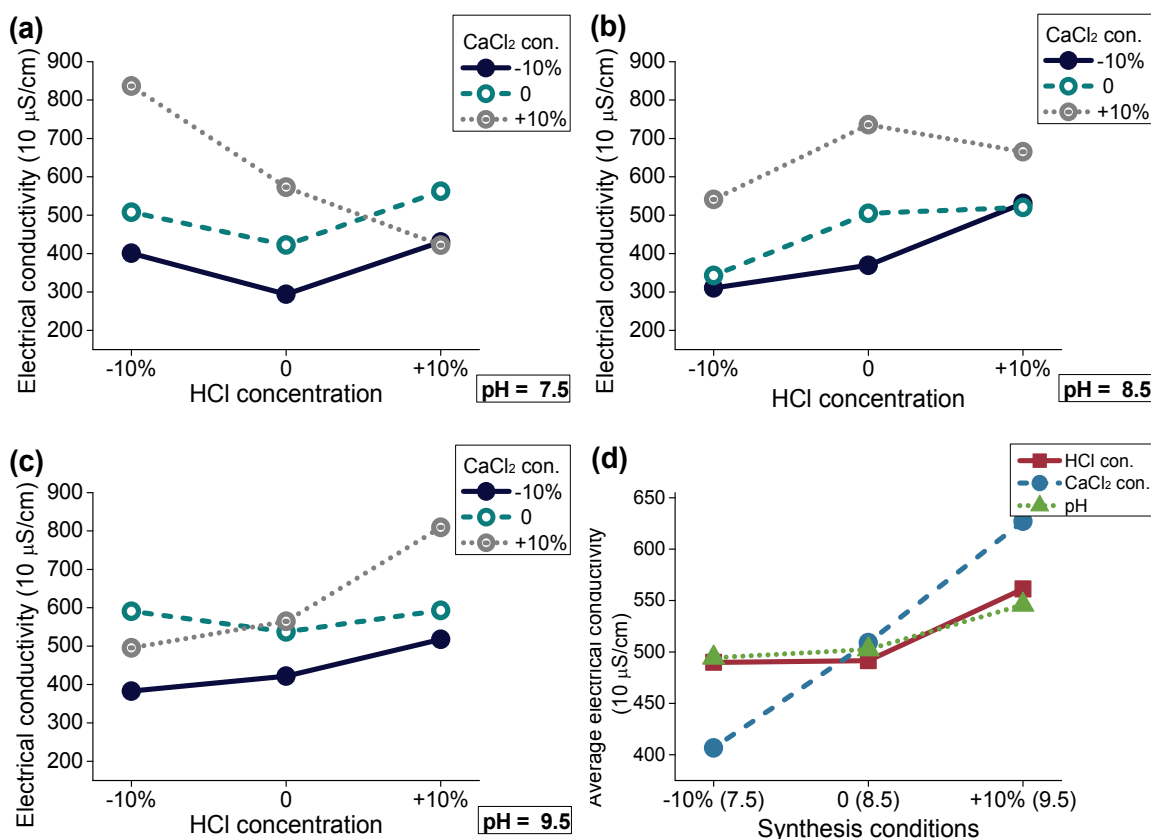


Figure 3. Electrical conductivity, as a function of synthesis conditions.

8.5 and 9.5, respectively).

Electrical conductivity reflects the amount of total dissolved ions from the pigment complex in solution. The conductivity values can be used to explain the solidification behavior of metal-salt complexes because ions trapped during solidification could be an origin of conductivity.

High content of ion concentrations in pigment solution can make ink spread into liquid media during printing. We assessed the effects of synthesis process parameters such as HCl and CaCl<sub>2</sub> concentrations and pH on the ion concentration.

For most of the conditions in Figures 3a, 3b, and 3c, electrical conductivity values increased with increments in HCl and CaCl<sub>2</sub> concentrations, even though a decrease was observed at high CaCl<sub>2</sub> concentration at pH 7.5 with HCl concentration increases.

The conductivity increases might be due to the influence of ions originating from HCl or CaCl<sub>2</sub>.

In Figures 3a, 3b, and 3c, the principal factor affecting the electrical conductivity of the pigment suspension was the CaCl<sub>2</sub> concentration during the coupling process. Increments in conductivity with HCl concentration or pH value were changed in the range 100-200 (10 $\mu$ S/cm), and those with CaCl<sub>2</sub> concentration were changed in the range 200-300 (10 $\mu$ S/cm). The mean values of the conductivities in Figures 3a, 3b, and 3c, were calculated and displayed in Figure 3d.

The mean value is the average conductivity of all samples having alterable experimental conditions, here for example pH or CaCl<sub>2</sub>, with one fixed experimental condition, here for example HCl. The fixed experimental condition was either pH or CaCl<sub>2</sub>, and the variable conditions were CaCl<sub>2</sub> and HCl, or HCl and pH, respectively. The adoption of the average value enabled us to estimate which parameter was most effective in electrical conductivity control.

In Figure 3d, the trends for the average conductivity values with HCl concentration and pH were nearly identical with very little changes.

The conductivity with CaCl<sub>2</sub> concentration increases

in a good linearity and a big amount. The increment of the average conductivity was more than 220 (10 $\mu$ S/cm) upon a 10% increment in CaCl<sub>2</sub> concentration. As explained above, CaCl<sub>2</sub> plays a decisive role in the precipitation of pigment in water media. Because the SO<sub>3</sub><sup>-</sup> and CO<sub>2</sub><sup>-</sup> anions in a pigment complex molecule are chelated by one Ca<sup>2+</sup> ion, an adequate mole ratio of CaCl<sub>2</sub> is important to achieve complete salt formation. When we add more CaCl<sub>2</sub> than a stoichiometric ratio of chelation, surplus Ca<sup>2+</sup> ions could be adhere on the surface of pigments or trapped in pigment solid, and they could be released into water for electrical conductivity measurement.

The conductivity increases with HCl or CaCl<sub>2</sub> concentration could have resulted from the increased free ions that separated from the pigment complex during conductivity measurement experiments.

However, the reason for the increased conductivity with pH value might be the ionic interaction changes via the ion exchange of protons for sodium ions in the pigment. "Lake" formation takes place initially in solution followed by nucleation and crystal growth, and subsequently, the reaction continues by a process of ion exchange in the crystal lattice<sup>4)</sup>. The pH could influence the last stage at which the metal exchange takes place, which is why the tendency for "lake" formation of the pigment using different molar ratios of HCl or CaCl<sub>2</sub> was changeable, depending upon pH control during the coupling reaction. At lower pH, the ratio between the bound calcium cations and the available sulfonate/carboxylate groups is reduced because of partial protonation of the binding sites<sup>20)</sup>. When all the strong acid groups, such as sulfonates, are paired with calcium ions and neutralized, the weaker acid groups, the carboxylates, will begin to associate with calcium ions<sup>19,22)</sup>. This general effect explains that the carboxylate group will be protonated more as the pH is reduced, with only the sulfonate group being ionized<sup>23)</sup>.

The monosodium and disodium salts would be formed together initially, with the intermediate species

involved in the conversion to the  $\text{Ca}^{2+}$  salt<sup>20</sup>). They might have different solubility characteristics, due to different Ca-complexing capacities as a function of the pH, directly effecting complex nucleation and growth mechanisms. This might possibly make the pigment particles become aggregate into larger as well as heterogeneous in size.

The solidification during precipitation at lower pH can be explained as a result of not only decreased conductivity, but also increased particle/aggregate size, as well as a decreased  $L^*$  value (whiteness).

The increase in particle size could be understood as crystallization and aggregation or agglomeration of particles<sup>24</sup>). The relationship between the particle size/morphology and the color change will be discussed in greater detail later. The conductivity increment with pH value might be caused by sodium ions trapped during the conversion process of the Na-salt form to the Ca-lake form.

The effect of proton concentration resulted in a different mechanism, comparing pH 7.5 with pH 9.5

in Figures 3a and 3c. The conductivity values increased in proportion to the HCl concentration at higher pH, but not at lower pH.

This may have occurred because the reduced proton concentration enhanced the dissociation of HCl, whereas the increased proton concentration could repress the dissociation of HCl. The conductivity dependence on  $\text{CaCl}_2$  concentration, however, might not be affected by pH value, because  $\text{Ca}^{2+}$  ions are not involved with protons directly. Increments in  $\text{CaCl}_2$  concentration increased the conductivity regardless of the pH. These patterns were reflected in the mean values of the conductivity in Figure 3d. An unusual decreasing pattern of conductivity with HCl concentration increases was revealed, particularly with a +10% concentration of  $\text{CaCl}_2$  at pH 7.5, in Figure 3a. During Ca-pigment complex formation, increased protonation at both the sulfonate and carboxylate groups could accelerate the insolubilization of the pigment to express the lowest conductivity. This result matched well with the data

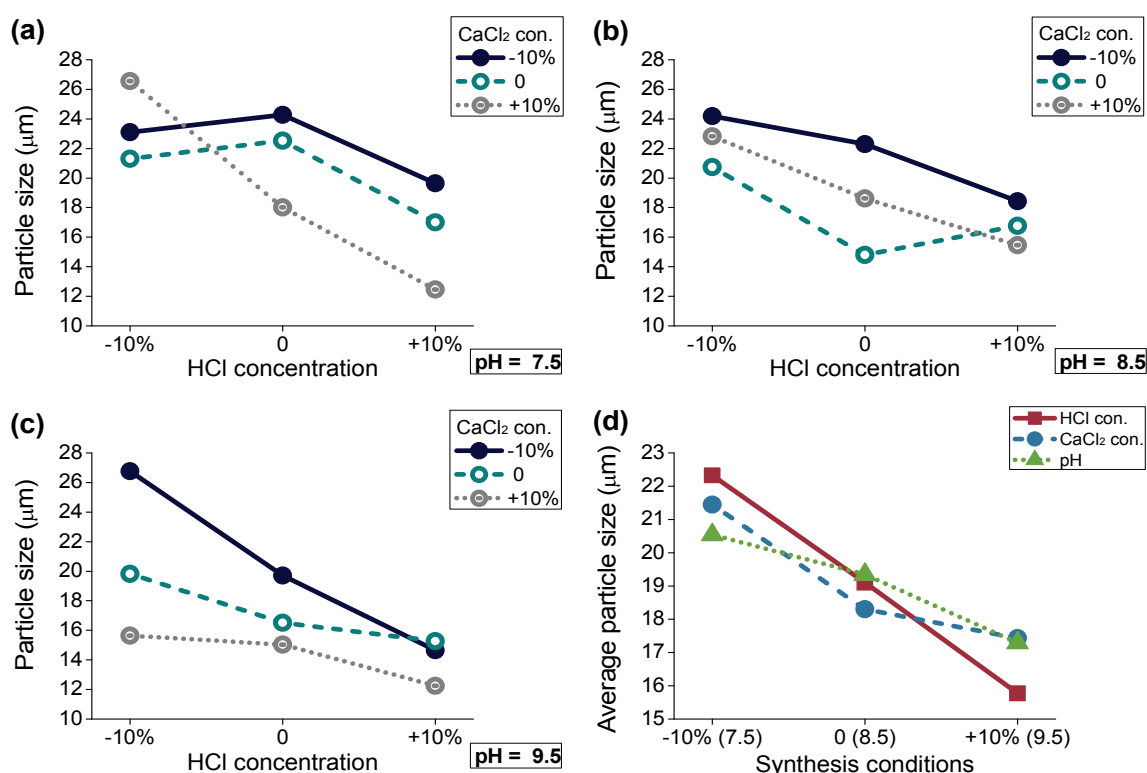


Figure 4. Particle size variation, as a function of synthesis conditions.



demonstrating that the lower pH concentration resulted in the lower conductivity (Figure 3d).

Considering the conductivity results, the  $\text{CaCl}_2$  concentration was confirmed as the key factor for controlling electrical conductivity.

The best conditions for the lowest conductivity (294.3 in Figure 3a) were the standard HCl concentration, a 10% reduction in the  $\text{CaCl}_2$  concentration, and pH 7.5. The conductivity value of 294.3 was almost half of the value (504.7) that was obtained under the standard conditions for all three experimental parameters.

Different concentrations of HCl and  $\text{CaCl}_2$  during the synthesis process changed the particle size at pH 7.5, 8.5 and 9.5, as shown in Figures 4a, 4b, and 4c, respectively.

Pigment particle size has a significant effect on the physical properties of a pigment. Changes in the particle size and particle size distribution are important considerations in assessing subsequent color alterations in pigments<sup>1,15</sup>. The particle size variation in this study was characterized in terms of particle aggregate size.

In Figures 4a, 4b, and 4c, the particle size decreased with increases in HCl and  $\text{CaCl}_2$  concentrations under different pH conditions, meaning the reduction in size of the particle aggregates (or agglomerates). This might be due to the increased ion numbers that resulted from the higher concentration of HCl or  $\text{CaCl}_2$ .

The concentration of HCl could affect the coupling reaction rate of the diazonium compound. With an increased number of  $\text{NO}^+$  ions due to increasing acid concentration, additional positively polarized diazonium ions would be available for the diazotization of the amines to increase the rate of the coupling reaction<sup>19</sup>. This mechanism might synergize the possibility of solidification with a smaller particle size resulting in smaller aggregates. With an increased  $\text{CaCl}_2$  concentration (more than one equivalent), surplus  $\text{Ca}^{2+}$  ions may increase the number of crystal nuclei during crystallization through chelation by calcium. Generally, in crystallization mechanism, increased numbers

of nuclei can reduce crystal size<sup>24</sup>.

The main effect of the individual parameters on particle size was estimated by the mean particle size values in Figure 4d. A negative linear relationship was revealed most strongly between the particle size and HCl concentration, indicating that the change of HCl concentration can effectively control the aggregate size.  $\text{CaCl}_2$  concentration and pH value exhibited good negative correlation with particle aggregate size as well. The decrement range of the average particle size with HCl concentration was about  $7\mu\text{m}$ , and that with  $\text{CaCl}_2$  or pH was about  $3\text{--}4\mu\text{m}$ . A 10% increase in HCl concentration from the standard conditions was the most effective in reducing particle aggregate size.

The pigment particle size variation were observed by the scanning electron microscopy (SEM) in Figure 5a, 5b, and 5c; which show the examples in which the particle aggregates with +10% increases in HCl,  $\text{CaCl}_2$  concentrations and pH were smaller.

The samples with HCl concentrations in Figure 5a showed relatively fine size in the aggregation/agglomeration levels, suggesting that higher HCl concentration was an important component in size control of the aggregates.

The particle aggregate size reduction as a result of pH value increase could be explained by a protonation mechanism on the potential ligands during conversion into the calcium salt form.

The precipitation via protonation at lower pH should be separate from the crystallization via calcium chelation in the pigment complex at higher pH.

If protonation occurred at calcium binding sites at lower pH, the pigments would be in an adverse condition for Ca-chelating complex formation because of the different protonation rates between  $\text{CO}_2^-$  and  $\text{SO}_3^-$  groups in the molecules.

Also, the coupling reaction between the weakly negative substituted diazonium component and the coupling component that does not possess adequate electronegativity would proceed very slowly<sup>19</sup>.

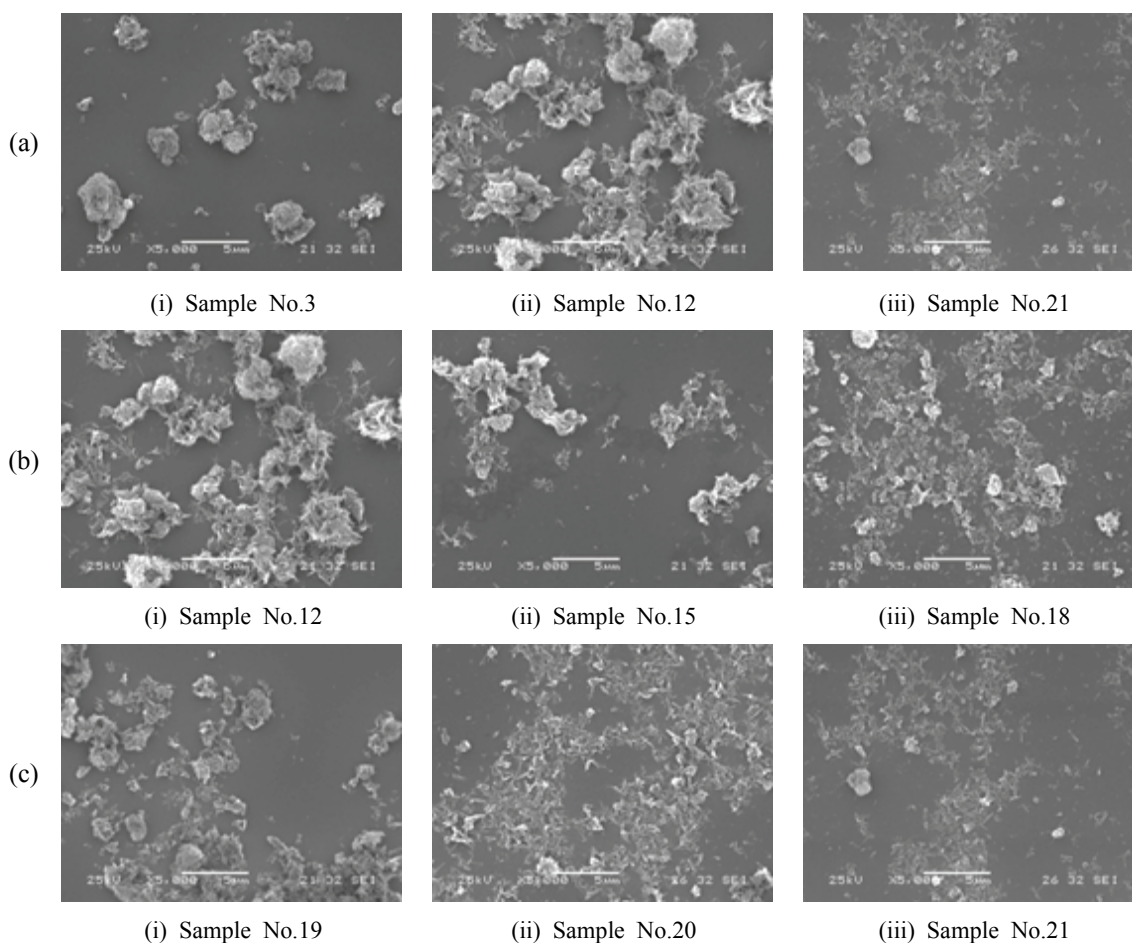


**Figure 5.** Scanning electron micrographs ( $\times 5000$ ) of pigment samples, showing aggregate patterns as a function of (a) HCl and (b)  $\text{CaCl}_2$  concentrations, and (c) pH condition.

The effect of the slower reaction would be to increase the heterogeneous nucleation and agglomeration of particles, and finally, to make the precipitates larger. During this process, large and small particles could easily coexist.

The smaller particle size at higher pH might be attributed to the development of crystallization via chelation by calcium. Due to more deprotonated  $\text{Ca}^{2+}$  salt-forming groups, the pigment could undergo a rapid coupling process and have higher capacity to convert disodium salts into calcium lakes.

The rapid reaction might render the formation of relatively small and uniform particles, resulting in smaller aggregates. The particle sizes of the pigments resulting from the various synthetic conditions were between 12 and 26  $\mu\text{m}$ .

The smallest particle size, 12.25  $\mu\text{m}$ , was obtained at pH 9.5 with +10% increases in both HCl and  $\text{CaCl}_2$  concentrations. This is obviously not the size of the primary particles (of the individual pigment crystals), but the size of the agglomerates and aggregates.

Practically in ink production, the pigment is dispersed into almost its primary particle, i.e., the agglomerates and aggregates are destroyed, through mechanical process such as grinding or milling.

Size reduction and color characteristics via milling process will be discussed further in our next paper in this series. The characteristic of pigment particles before milling is turned to be a distinct factor to determine particle size and color of pigment after milling in the series work. That is why we have to understand the particles shape and properties before

treatment such as milling or surface treatment.

Consequently, the  $\text{CaCl}_2$  concentration strongly affected the lowering of the ion conductivity, and the HCl concentration is so effective to control the particle aggregate size. To produce a pigment having lower conductivity and smaller particle size, the amount of  $\text{CaCl}_2$  should be reduced by 10% from the standard, and the HCl concentration should be increased by 10% in this experimental.

Even the chemically identical pigments can show diverse color as a result of different synthesis conditions, because so many morphological aspects of the pigment affect the colorimetric properties. Different particles aggregate sizes and the size distributions can change the color characteristics of these pigments, such as brightness, intensity, shade, purity, and depth.

The color characteristics of the pigments prepared under different HCl and  $\text{CaCl}_2$  concentrations and pH conditions were investigated by measuring  $L^*a^*b^*$  values in painted films of the pigments, and the results are recorded in Table 2.

The mean values of  $a^*$ ,  $b^*$  and  $L^*$  were calculated to observe the effect of each synthesis parameter on the color characteristics. The mean values of  $a^*$ ,  $b^*$  and  $L^*$  are shown in Figures 6a, 6b, and 6c, respectively. The chromatic difference values ( $\Delta E$ ) were also evaluated for color quality control on the

basis of the color value of pigment sample No.14 as a standard. The patterns of the mean value of  $\Delta E$  are shown in Figure 6d.

In Figures 6a and 6b, both  $a^*$  (redness) and  $b^*$  (yellowness) values tended to increase with an increase in HCl concentration. They increased particularly between -10% and the standard HCl concentration conditions. When the HCl concentration was increased to +10%, there were no significant changes in  $a^*$  and  $b^*$  values; indeed, there was a slight drop in the  $b^*$  value. This meant that the HCl concentration could be controlled to at least the standard amount for an intense yellower-red coloring, as well as decreased to -10% for a better bluer-red hue, compared to the current pigment. When the  $\text{CaCl}_2$  concentration for the coupling component was raised to +10%, the pigment exhibited a slightly yellower-reddish color, as shown by the slightly decreased  $a^*$  and increased  $b^*$  values. If the pH was controlled as high as 9.5 during the coupling reaction, the reddish shade of the pigment diminished gradually and had a somewhat more bluish shade, with the decreased patterns in both  $a^*$  and  $b^*$  values. The effect of HCl concentration on both  $a^*$  and  $b^*$  values appeared most prominently.

The  $\text{CaCl}_2$  concentration and pH conditions seemed not to affect either  $a^*$  or  $b^*$  values in comparison to the HCl concentration.

**Table 2.** Color characteristics ( $L^*a^*b^*$  values) of variously synthesized pigments

No.	$L^*$	$a^*$	$b^*$	No.	$L^*$	$a^*$	$b^*$	No.	$L^*$	$a^*$	$b^*$
1	26.1	47.2	30.9	10	27.4	49.9	33.9	19	28.8	50.4	21.6
2	29.4	42.7	18.1	11	26.7	50.0	34.3	20	29.2	50.0	31.9
3	24.3	45.5	29.7	12	27.8	49.3	32.0	21	27.9	49.3	33.2
4	27.9	44.2	25.9	13	29.2	48.7	30.2	22	27.7	50.0	32.3
5	26.3	45.4	28.5	14	28.4	49.5	31.3	23	28.4	50.9	33.1
6	28.9	40.3	21.7	15	27.0	47.9	30.7	24	28.9	47.4	28.8
7	26.3	45.7	27.3	16	27.1	49.8	33.0	25	27.2	51.1	34.8
8	29.9	45.2	27.4	17	27.2	49.1	31.9	26	29.5	47.8	30.0
9	26.5	46.4	28.4	18	26.7	48.0	31.7	27	24.5	48.4	33.4

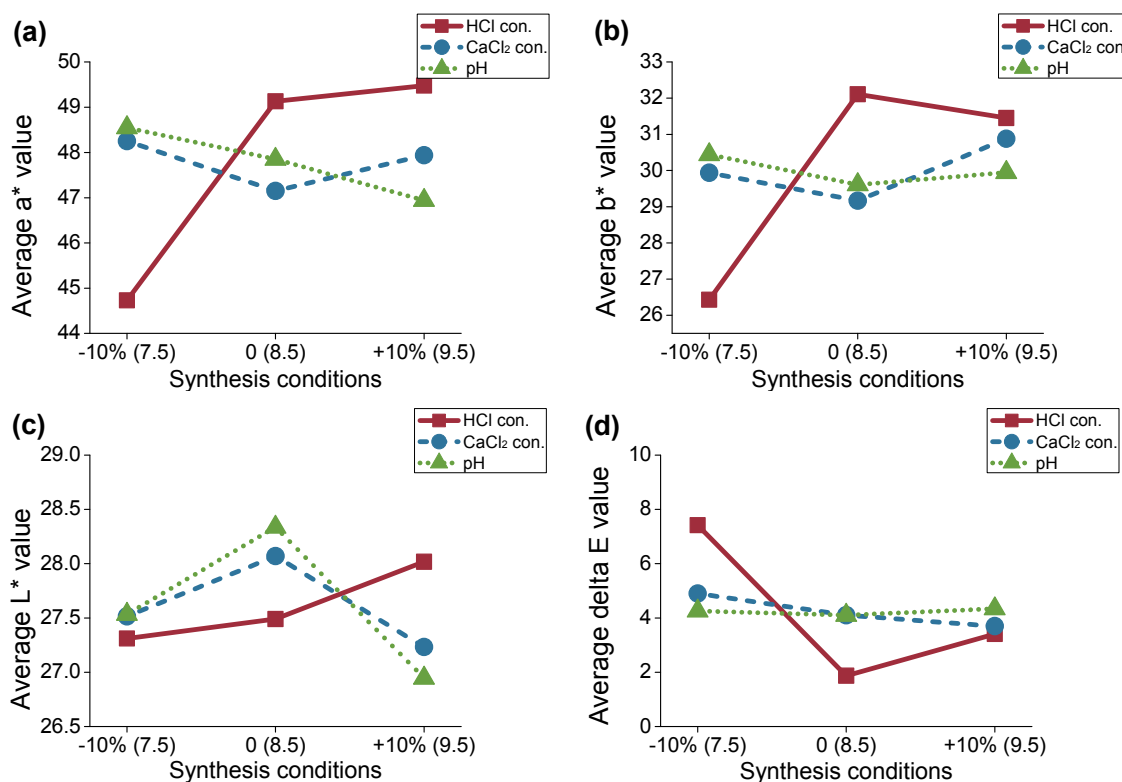


Figure 6. Average  $a^*$ ,  $b^*$ ,  $L^*$  and  $\Delta E$  values, as functions of synthesis conditions.

The increase in both the average  $a^*$  and  $b^*$  values with HCl concentration recorded was about 5 values. The extent of change in the average  $a^*$  and  $b^*$  values with  $\text{CaCl}_2$  concentration or pH was about 0.5-1.5 values.

In Figure 6c, the average  $L^*$  (whiteness) value also increased, particularly with HCl concentration. Neither the  $\text{CaCl}_2$  concentration nor the pH value appeared to result in a certain trend in the average  $L^*$  values. Changes of  $\pm 10\%$  for both from the standard conditions resulted in reduced  $L^*$  values. These findings might have been caused by heterogeneous particle size distributions.

The color changes toward improved red and yellow tones with higher whiteness upon increased HCl concentration might have been due to the decreased particle aggregate size of the pigment. Particle/aggregate size can influence the opacity, color strength, and hue of pigments.

Not only the particle size, but also the particle size distribution, can provide important information to control

the color characteristics of pigments. Small and uniform particles provide greater tinting strength and purer color<sup>26)</sup>. Larger and heterogeneously sized particles or aggregates allow more diverse light to pass through the layer of painted film to be reflected from the ground, thereby increasing its chromatic diversity<sup>25)</sup>. For example, pigment particles of about one micron in size have a distinct violet tint, differing from the bright red color of sub-micron particles<sup>27,28)</sup>.

Figure 7 shows an example of particle size distribution curves for the pigment samples with 10% increase in only one parameter while holding other two parameters at standard conditions.

In Figure 7, sample No. 23 that synthesized with 10% increase of HCl concentration showed a narrower distribution curve of particle aggregate size compared with the sample No. 15 and 17 which synthesized with increases in the coupler components, i.e., pH and  $\text{CaCl}_2$  concentration, respectively. The HCl concentration increment strongly influenced the reduction of particle aggregate size and a narrow size distribut-

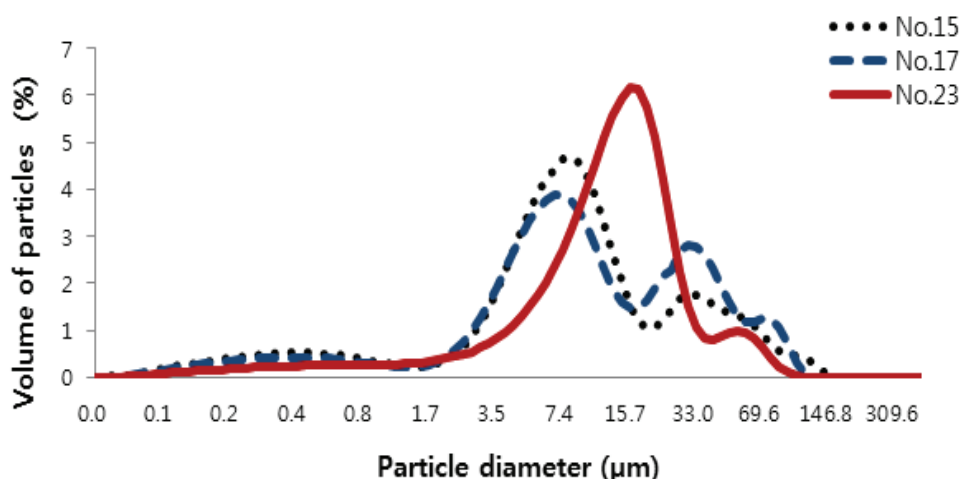


**Figure 7.** Particle size distribution of pigment samples (No. 15 sample was synthesized under pH 9.5 and standard  $\text{CaCl}_2$  and HCl concentrations. No. 17 sample was synthesized under pH 8.5 and standard HCl concentration with 10% higher concentration of  $\text{CaCl}_2$ . No. 23 sample was synthesized under pH 8.5 and standard  $\text{CaCl}_2$  concentration with 10% higher concentration of HCl).

ion in the present study.

Smaller aggregates with uniform sizes as a result of the HCl concentration increment might contribute to the shift of the pigment color into strong reddish and yellowish shades, i.e., the purer hue of a brilliant red color, with higher  $a^*$ ,  $b^*$ , and  $L^*$  values. Increments in the  $\text{CaCl}_2$  concentration or pH also resulted in smaller aggregate sizes, but the particle size distributions were practically extended. The small but heterogeneous particles which were extensively aggregated caused the pigment to be darker, bluer, and less reddish in color.

The pigments should not exhibit significant color

differences with the synthesis condition changes that lower electrical conductivity or reduce particle size. However,  $\Delta E$  results for the pigment appeared to be influenced by the different synthesis conditions, as shown in Figure 6d.

In the figure, the average  $\Delta E$  values showed a significant increase with a  $-10\%$  change in HCl concentration.

The decreased HCl concentration resulted in a large color difference in the pigment compared to the standard pigment sample, No. 14.

The yellower-red pigments with increased HCl concentration had little color difference, but the blue

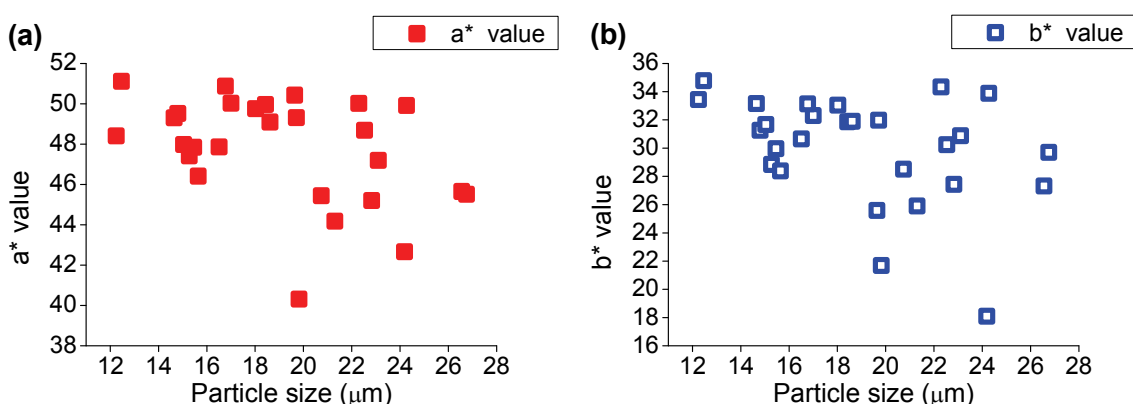


**Figure 8.** Scatter plots of particle size vs  $a^*$  and  $b^*$  values of synthesized pigments.

-shifted red pigments with decreased HCl concentration signified a great color difference.

The drop in  $b^*$  values might be the very direct cause that brought about the color divergence<sup>29)</sup>. The average  $\Delta E$  value resulting from  $\text{CaCl}_2$  or pH parameter changes was only slightly affected.

The pigments with different  $\text{CaCl}_2$  concentrations or pH values during the coupling process nearly retained their quality.

The modification of HCl concentration could be detrimental to maintaining pigment quality, but even favorable with respect to the pigment handling for various coloring purposes.

Interestingly, all the average  $\Delta E$  data were positioned in the range 3.4-4.3, with the individual parameter increments of +10%. The convergence of  $\Delta E$  might indicate that no matter which parameter was increased by 10%, the final color change would appear similar. Because the color characteristics of pigments can be often interpreted with respect to their particle size, the role of HCl concentration in pigment color changes can be ascertained from Figure 4.

The increased HCl concentration strongly influenced the particle aggregate size reduction as well as the deviation of  $\Delta E$  values. To support the correlation between the particle aggregate size and color changes, plots of particle aggregate sizes versus  $a^*$  or  $b^*$  values for all the samples are described in Figure 8, to buttress the  $\Delta E$  data in Figure 6d.

In Figure 8, both  $a^*$  and  $b^*$  values were positioned at higher value levels and converged, as the particle aggregate size decreased. With increasing particle aggregate sizes, both  $a^*$  and  $b^*$  values spread and became lower at high declination. This pattern was observed in Figure 6d, which showed a sharp increment in  $\Delta E$  as a result of decreased HCl concentration, and was accompanied by a rapid increase in aggregate size, as seen in Figure 4.

This confirmed the resultant reddish as well as yellowish color changes of the smaller aggregate-sized pigments.

## 4. Conclusion

Significant differences in the characteristics of azo pigment particles of PR 57:1 were observed, depending on the synthesis conditions, with an emphasis on the alteration of particle (aggregates or agglomerates) size and colorimetric features. We deduced the optimal synthesis conditions from various experiments with changes in three parameters: controlling the amount of HCl during the diazo reaction, and  $\text{CaCl}_2$  concentration and pH during the coupling reaction to synthesize the pigment.  $\text{CaCl}_2$  concentration had the biggest influence to electrical conductivity control. HCl concentration had the highest impact on the particle aggregate size and color characteristics.

The normal magenta color of the pigment was changed to brighter reddish and more yellowish shade with lower color differences,  $\Delta E$ , when the higher HCl concentration was applied. A stronger bluish, less reddish, and darker red color with a higher color difference,  $\Delta E$ , was exhibited with a lower HCl concentration.

The HCl concentration might be one of key factors to maintain the pigments color characteristics through morphological features controlling such as particle aggregate size and size distribution. We observed the correlations between pigment particle aggregate size and color changes in PR 57:1.

The most promising manufacturing conditions for producing pigments with low ion conductivity were proposed. And it was understood that how those conditions can change particle aggregate size and color characteristics even though the produced pigment is not ready for applications. The pigment particle morphology such as primary particle size and state of dispersions from agglomerates/aggregates are relevant for the pigment quality and color characteristics for applications.

It has been known that this can be achieved via a mechanical milling process, and we will be discussed about this matter in the next series work.

## Acknowledgements

This work was supported by a grant from the Fundamental R&D Program for Core Technology of Materials and the Materials and Components Technology Development Program (10047681, Development of low cost conductive paste capable of fine pattern for touch panel and high conductivity for solar cell using metal composite with core-shell structure prepared by highly productive wet process), which is funded by the Ministry of Trade, Industry and Energy (MI, Korea).

## References

1. W. Herbst and K. Hunger, "Industrial Organic Pigments: Production, Properties, Applications, 3rd ed.", Wiley-VCH, Weinheim, 2004.
2. T. E. Ludwig, 'Rubines', In: T. C. Patton, "Pigment Handbook, Volume 1, Properties and Economics, 1st ed.", Wiley, New York, p.505, 1973.
3. P. A. Lewis, 'Colored Organic Pigments', In: J. V. Koleske, "Paint and Coating Testing Manual: Fourteenth Edition of the Gardner-sward Hand-book", American Society for Testing Materials (ASTM) International, Chap.21, p.192, 1995.
4. R. M. Christie and J. L. Mackay, Metal Salt Azo Pigments, *Coloration Technology*, **124**(3), 133 (2008).
5. H. Zollinger, "Color Chemistry: Synthesis, Properties and Applications of Organic Dyes and Pigments, 2nd ed.", VCH, Weinheim, 1991.
6. A. R. Kennedy, C. M. Nair, W. E. Smith, G. Chisholm, and S. J. Teat, The First Red Azo Lake Pigment Whose Structure is Characterized by Single Crystal Diffraction, *Angewandte Chemie International Edition*, **39**(3), 638(2000).
7. C. Gmbh, U.S. Pat. 6159649(2000).
8. W. S. Czajkowski, 'Organic Pigments', In: A. T. Peters, H. S. Freeman, "Modern Colorants: Synthesis and Structure, Advance in Color Chemistry Series, Volume 3", Springer Science and Business Media, LLC, New York, Chap.3, pp.63-65, 1995.
9. K. Supattarasakda, K. Petcharoen, and T. Perm-pool, Control of Hematite Nanoparticle Size and Shape by the Chemical Precipitation Method, *Powder Technology*, **249**, 353(2013).
10. R. M. Christie and S. Moss, Metal Salt Azo Pigments Derived from 3-hydroxy-2-naphthohydr-oxamic Acid, *Dyes and Pigments*, **8**(3), 211 (1987).
11. R. A. M. C. D. Groote and M. G. Neuman, Spot Test for Azo Dye Formation, *J. of Chemical Education*, **56**(9), 625(1979).
12. I. M. Arabatzis, S. Antonaraki, T. Stergiopoulos, A. Hiskia, and E. Papaconstantinou, Preparation, Characterization and Photocatalytic Activity of Nanocrystalline Thin Film TiO<sub>2</sub> Catalysts towards 3,5-dichlorophenol Degradation, *J. of Photochemistry and Photobiology A: Chemistry*, **149**(1-3), 237 (2002).
13. R. W. G. Hunt and M. R. Pointer, "Measuring Colour, 4th ed.", John Wiley and Sons, Ltd., UK, p.57, 2011.
14. R. K. Harris, P. Jonsen, K. J. Packer, and C. D. Campbell, Investigation of the Structure of an Insoluble Pigment by Means of Nuclear Magnetic Resonance, *J. of the Chemical Society, Perkin Transactions*, **2**(10), 1383(1987).
15. Z. Hao and A. Iqbal, Some Aspects of Organic Pigments, *Chemical Society Reviews*, **26**(3), 203 (1997).
16. S. L. Bekö, S. M. Hammer, and M. U. Schmidt, Crystal Structures of the Hydration States of Pigment Red 57:1, *Angewandte Chemie International Edition*, **51**(19), 4735(2012).
17. G. R. Duckett, J. R. Fryer, and T. Baird, Electron Microscope Studies of a Mono-azo Pigment, Electron Microscopy and Analysis, Proceedings of the Institute of Physics Electron Microscopy and Analysis Group Conference Held at the University of Newcastle-upon-Tyne, 2-5 September 1985 (EMAG 85), Adam Hilger, Vol.78, p.437, 1985.
18. R. T. Buwalda, J. M. Jonker, and J. B. F. N. Engberts, Aggregation of Azo Dyes with Cationic Amphiphiles at Low Concentrations in Aqueous Solution, *Langmuir*, **15**(4), 1083(1999).
19. E. N. Oparah, Synthesis of Acid Azo Dyes based

- on 6-amino-1-naphthol-3-sulphonic Acid and the Assessment of their Properties on Nylon, Wool and Leather, Ph.D. Thesis, Ahmadu Bello University, 2010.
20. R. M. Christie, I. Chugtai, and R. R. Mather, The Influence of Synthesis Conditions on the Crystal and Aggregate Properties of Calcium Salt Azo Pigment C.I. Pigment Red 48: 2, *Dyes and Pigments*, **80**(2), 264(2009).
  21. J. S Bae, S. Y. Gwon, and S. H. Kim, Anthraquinone-carbamodithiolate Assembly as Selective Chromogenic Chemosensor for  $Fe^{3+}$ , *Textile Coloration and Finishing*, **25**(1), 13(2013).
  22. E. Fourest and B. Volesky, Contribution of Sulfonate Groups and Alginate to Heavy Metal Biosorption by the Dry Biomass of *Sargassum fluitans*, *Environmental Science and Technology*, **30**(1), 277(1995).
  23. A. Navarro and F. Sanz, Dye Aggregation in Solution: Study of C.I. Direct Red I, *Dyes and Pigments*, **40**(2-3), 131(1999).
  24. F. Wang, V. N. Richards, S. P. Shields, and W. E. Buhro, Kinetics and Mechanisms of Aggregative Nanocrystal Growth, *Chemistry of Materials*, **26**(1), 5(2014).
  25. J. E. Otterstedt and D. A. Brandreth, "Small Particles Technology", Springer Science and Business Media, LLC, New York, p.212, 1998.
  26. H. E. Merwin, Optical Properties and Theory of Color of Pigments and Paints, American Society for Testing Materials(ASTM) Proceedings, USA, Vol.17, No.2, p.494, 1917.
  27. <http://www.naturalpigments.com/art-supply-education/traditional-oil-painting-revival/2013.10.06>.
  28. D. Hradil, T. Grygar, J. Hradilová, and P. Bezdička, Clay and Iron Oxide Pigments in the History of Painting, *Applied Clay Science*, **22**(5), 223(2003).
  29. H. Jung and T. Sato, Comparison between the Color Properties of Whiteness Index and Yellowness Index on the CIELAB, *Textile Coloration and Finishing*, **25**(4), 241(2013).